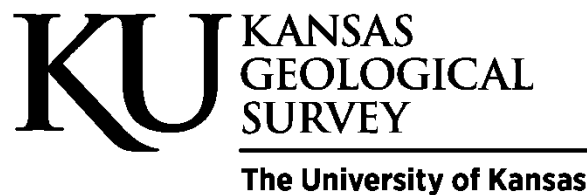


Critical Minerals Enrichment in Pennsylvanian Black Shales of Kansas

By Sahar Mohammadi, Jon Smith, Kate Andrzejewski, Stephan Oborny,
Alan Peterson, Precious Oso, and Theodor Lowe

*Kansas Geological Survey Open-File Report No. 2026-24
May 2026*



1930 Constant Ave., Lawrence, KS 66047 (785) 864-3965; www.kgs.ku.edu

Critical Minerals Enrichment in Pennsylvanian Black Shales of Kansas

Sahar Mohammadi, Jon Smith, Kate Andrzejewski, Stephan Oborny,
Alan Peterson, Precious Oso, and Theodor Lowe

1. Introduction

This research contributes to the U.S. Geological Survey (USGS) Earth Mapping Resource Initiative by focusing on the geochemical characterization of critical minerals in Pennsylvanian black shales of eastern Kansas within the Cherokee-Forest City Basin. These fine-grained, organic-rich sedimentary rocks were deposited in marine or restricted basin environments and are known hosts for elements such as nickel (Ni), cobalt (Co), molybdenum (Mo), and vanadium (V) (Vine and Tourtelot, 1969; Mastalerz et al., 2020). These metals, along with rare earth elements (REEs), are essential to the clean energy transition (Emsbo et al., 2015; Olivetti et al., 2017).

The Kansas Geological Survey (KGS) serves as project lead within this multistate collaboration. In coordination with geological surveys from Illinois, Indiana, Iowa, Kentucky, Missouri, and Ohio, KGS developed a pilot work plan and standardized sampling protocols to ensure consistent collection, analysis, and reporting. By integrating new geochemical data from Kansas black shales with standardized sampling across multiple basins, this study aims to clarify patterns of mineral enrichment, evaluate depositional and diagenetic processes, and contribute to the national understanding of critical mineral potential in Paleozoic sedimentary rocks.

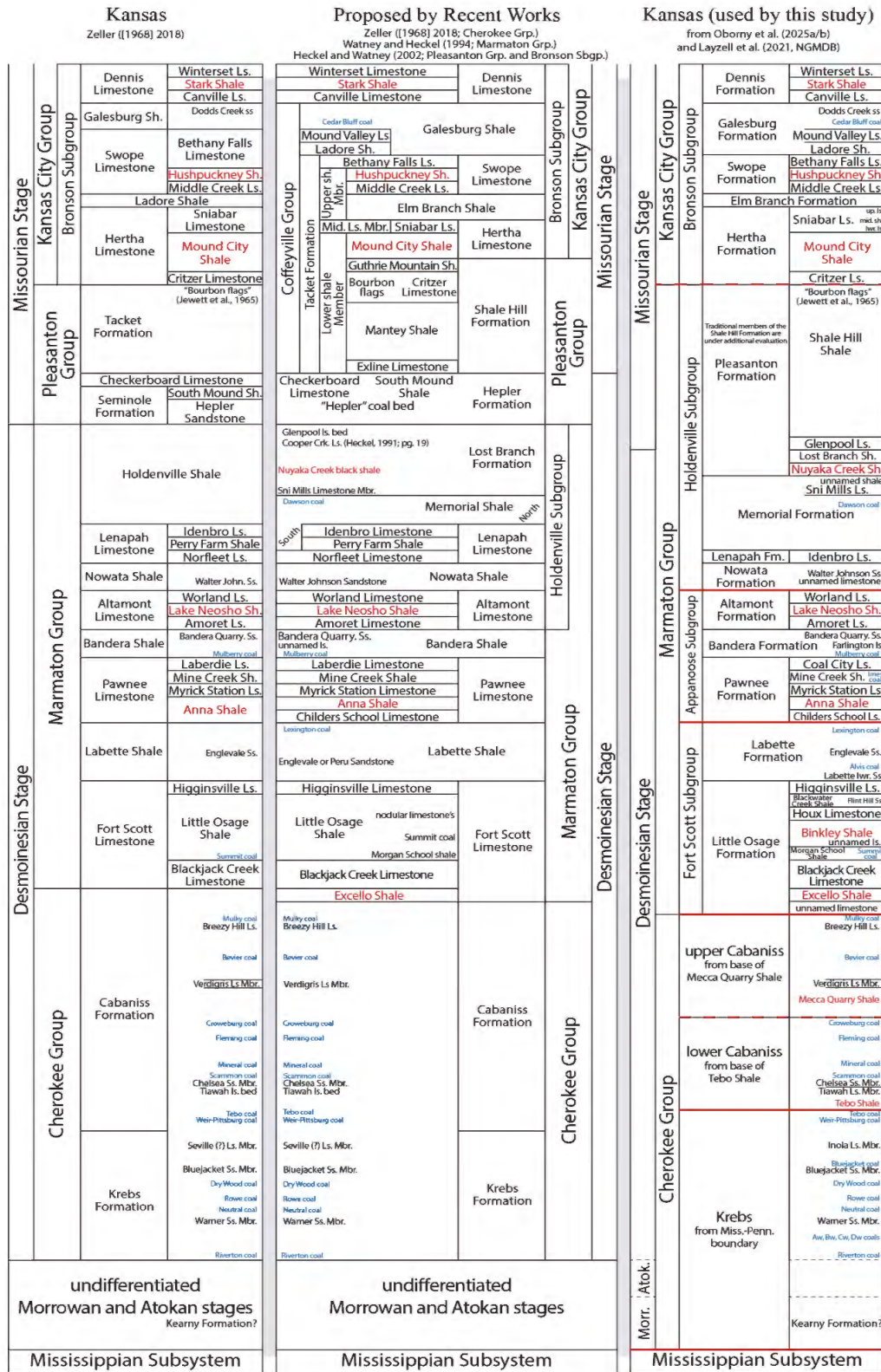


Figure 1. Pennsylvanian nomenclature of Kansas, modified from CoreCM, 2025b. Units shown in red indicate targeted shale intervals.

2. Methodology

2.1 Sampling

Eight organic-rich black shales were sampled from one outcrop and six drill cores, including Edmonds 1-A (Leavenworth County), D.C.C 1 (Douglas County), Hinthorn CW-1 (Montgomery County), PNR 1 (Linn County), PNR 2 (Bourbon County), and Tietjens 1-12 (Brown County), representing the upper Desmoinesian and lower Missourian Stages in eastern Kansas (fig. 2). All cores were obtained from the KGS Drill Core Library.

Samples from three cores (D.C.C 1, Edmonds 1-A, and Hinthorn CW-1) were analyzed using portable X-ray fluorescence (pXRF), inductively coupled plasma mass spectrometry (ICP-MS), total organic carbon (TOC), and sulfur content. In ascending stratigraphic order, the shale members studied include the Excello, Binkley (Little Osage), Anna, Lake Neosho, Nuyaka Creek, Mound City, Hushpuckney, and Stark members. These deposits are laterally extensive across the region, exhibit prominent gamma-ray responses exceeding 300 API, and consist of fine-grained, phosphatic, fissile black shales that are stratigraphically well constrained. The Stark Shale is absent in the PNR 1 and NPR 2 cores, where the Hushpuckney Shale occurs at the surface. Outcrop samples were collected at 1 cm resolution and sealed individually for pXRF analysis.

Four of the cores — PNR 1, D.C.C 1, Hinthorn CW-1, and Edmonds 1-A — were selected for further detailed study. These cores were described in detail for lithology, facies identification, and mineralogical characterization to interpret depositional and diagenetic processes influencing critical mineral distribution. Core descriptions include lithologic variations, grain composition, sedimentary structures, and diagenetic features.

Approximately 90 shale billets showing notable changes in color, texture, or composition were collected for thin-section preparation and petrographic analysis. Outcrop samples from Linn and Montgomery counties were also collected to complement core observations and overcome one-dimensional sampling limitations. Outcrop sections were measured systematically, and the size, shape, and spacing of phosphatic nodules were recorded to evaluate their role in mineral concentration.

Bulk and clay mineralogy were determined through X-ray diffraction (XRD) analysis. Powdered bulk samples were analyzed to identify and quantify mineral components, while the clay fraction (<2 μm) was separated and treated through glycolation, heating, and magnesium saturation to determine clay species and alteration stages, including smectite-to-illite transformation.

Focused scanning electron microscopy (SEM) coupled with energy dispersive spectroscopy (EDS) was used to investigate diagenetic mineral phases, textural relationships, and paragenetic

sequences. These high-resolution imaging and compositional analyses provided insights into mineral morphology, alteration processes, and environmental factors influencing the spatial distribution of critical minerals within the studied black shales.

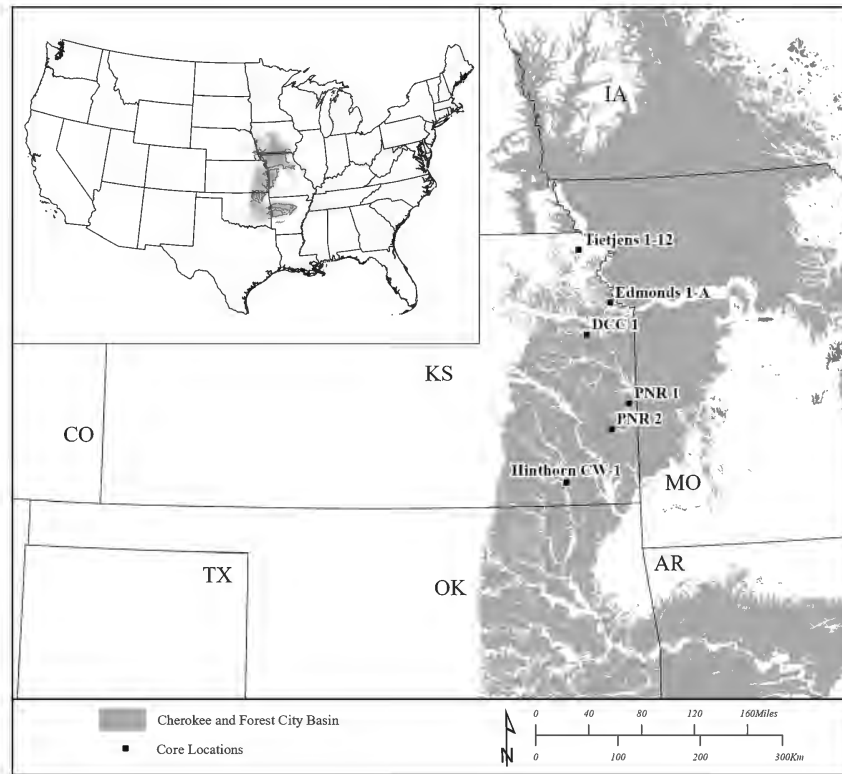


Figure 2. Kansas map showing sample locations for the study area.

2.2 Techniques

2.2.1 Portable X-Ray Fluorescence (pXRF)

Elemental analyses were performed at the KGS using an Olympus Vanta handheld energy-dispersive X-ray fluorescence spectrometer in Geochem (3-Beam) mode at a 1 cm sampling resolution. The instrument utilized an 8 mm beam for spot measurements. Samples were cleaned by hand-sanding with fine-grit sandpaper and wiped with Kimwipes to remove surface contamination prior to analysis. Calibration checks were performed before each analytical session using USGS-certified reference materials representing black shale, carbonate-rich shale, phosphate rock, soil, and carbonatite. Three beams were applied sequentially at 10, 40, and 50 kV, each for 40 seconds, yielding a total analysis time of 120 seconds per sample.

The pXRF analyses provided semi-quantitative concentrations of major and trace elements to evaluate geochemical variations within and between shale members. Measurements were validated against USGS reference materials, and all uncertainties were reported to three standard deviations.

2.2.2 Total Organic Carbon and Sulfur (TOC and S)

TOC and sulfur contents were analyzed on shale samples from PNR 1, PNR 2, and D.C.C 1 cores by the Indiana Geological and Water Survey using a Leco SC832DR elemental analyzer. Each powdered sample (~2 g) was combusted at 1350°C in a pure oxygen atmosphere, releasing carbon as CO₂ and sulfur as SO₂ gases. The evolved gases were measured in detection cells relative to calibration standards to determine total carbon (TC) and total sulfur (S) contents. Inorganic carbon (IC) was determined using a CM5017 coulometer coupled with a CM5330 acidification module, where carbonate species were converted to CO₂ for quantification.

Total organic carbon (TOC) was calculated by subtracting IC from TC. Average TOC and TOC/S ratios were determined for each shale member after removing statistical outliers. These analyses followed the standard carbon and sulfur determination methods routinely used by the Indiana Geological and Water Survey.

2.2.3 Inductively Coupled Plasma Optical Emission and Mass Spectrometry (ICP-OES/MS)

Based on pXRF results, a total of 355 shale samples were analyzed for elemental composition by USGS laboratories at SGS Natural Resources using SGS protocols. Samples were crushed and pulverized (<2 mm) to achieve homogeneity before digestion and analysis. For method GE_ICM91A50, samples were fused with sodium peroxide and dissolved in nitric acid for ICP-OES/MS measurement. For method GE_IMS21B20, samples were digested with a 3:1 mixture of HCl and HNO₃. Wavelength-dispersive X-ray fluorescence (WDXRF) analyses (method GO_XRF72) were conducted on fused disks to quantify major oxides and trace elements. These combined ICP and XRF results provided high-precision elemental concentrations used to calibrate and validate the pXRF data, assess trace element behavior, and evaluate enrichment patterns of critical minerals in the shales.

2.2.4 X-Ray Diffraction (XRD)

XRD analyses were conducted at the KGS using a Rigaku Miniflex 6G Benchtop X-ray Diffractometer to determine both bulk and clay mineralogy. All samples were run with an X-ray generator setting of 40kV and 15mA. Bulk samples were prepared as powder mounts and analyzed with a step scan

of .01° over a spectrum of 3°-90° 2θ. The <2 μm clay fraction was separated through dispersion in deionized water, centrifugation, and decantation per protocol methods used by the KGS Soil and Paleosol Laboratory. The clay fraction was then transferred onto glass slides and subjected to glycolation, heating at 500 °C for at least 2 hours, and magnesium saturation treatments prior to analysis. Oriented aggregate clay mounts were analyzed with a step scan of .01° over a spectrum of 2°-35° 2θ.

Mineral identification and quantification were conducted using the Rigaku SmartLab Studio II software in combination with the ICDD PDF-4 Mineral database. Quantification for mineral abundance was conducted using Rietveld analysis. Identified mineral phases include illite, smectite, kaolinite, apatite, zeolite, and associated phosphate minerals. The data provided insight into diagenetic processes, clay transformations (such as smectite-to-illite), and their relation to the occurrence of critical minerals.

2.2.5 Scanning Electron Microscopy and Energy Dispersive Spectroscopy (SEM-EDS) and Back-Scattered Electrons (BSE)

Scanning electron microscopy combined with energy dispersive spectroscopy was used to examine polished thin section samples in the Microscopy and Analytical Imaging Research Resource Core Laboratory at the University of Kansas, where a Hitachi S-4700 cold field emission scanning electron microscope was employed. Samples were first evaluated petrographically to choose areas of interest, then mounted on aluminum holders with conductive carbon adhesive and coated with a thin iridium layer to limit charging. Imaging was completed at a working distance of 12 mm using secondary and back-scattered electron detectors to observe surface textures and distinguish mineral phases, and energy dispersive spectroscopy was performed at 15 to 20 kV to obtain elemental maps that were processed with the Oxford Aztec software.

These analyses aim to determine diagenetic mineral phases, establish paragenetic sequences, and assess how critical minerals are influenced by or contribute to diagenetic alterations. The results will enhance understanding of mineral formation, elemental trapping mechanisms, and the fine-scale distribution of critical minerals in shale matrices.

3. Results

3.1 Concentrations of enriched critical minerals in Pennsylvanian black shales

The pXRF analyses revealed consistent enrichment of redox-sensitive trace metals across the studied cores, though magnitude and distribution varied by shale unit and stratigraphic position.

PNR 1 — Exhibited elevated concentrations of vanadium, nickel, zinc, and arsenic in the Hushpuckney and Nuyaka Creek shales. Vanadium values exceeded 2,600 ppm, and nickel reached over 1,000 ppm, while zinc concentrations surpassed 5,000 ppm. The Anna and Binkley shales also contained notable enrichments, while Mound City and Excello shales were generally lower in metal content.

PNR 1	Arsenic (As) (ppm)			Nickel (Ni) (ppm)		
	Min	Max	Average	Min	Max	Average
Stark	-	-	-	-	-	-
Hushpuckney	6	58	30	165	573	331
Mound City	3	36	7	50	1,009	170
Nuyaka Creek	11	141	53	56	601	337
Lake Neosho	-	-	-	-	-	-
Anna	4	60	147	76	654	267
Binkley	4	44	16	58	635	333
Excello	2	50	10	12	391	172

Table 1. Data showing arsenic and nickel content (range and average) in the studied shales from the PNR 1 core, measured with pXRF.

PNR 1	Vanadium (V) (ppm)			Zinc (Zn) (ppm)		
	Min	Max	Average	Min	Max	Average
Stark	-	-	-	-	-	-
Hushpuckney	198	2,662	1,311	370	5,277	1,886
Mound City	80	920	188	61	2,351	274
Nuyaka Creek	165	1,108	686	42	374	90
Lake Neosho	-	-	-	-	-	-
Anna	70	1,189	276	27	2,392	211
Binkley	94	2,057	849	126	5,847	2,010
Excello	78	986	304	12	605	256

Table 2. Data showing vanadium and zinc content (range and average) in the studied shales from the PNR 1 core, measured with pXRF.

PNR 2 — Showed similar enrichment patterns, though concentrations were generally higher. The Hushpuckney and Mound City shales recorded strong vanadium and chromium values, with vanadium above 2,000 ppm and chromium exceeding 1,400 ppm. The Binkley shale had the highest zinc concentrations, exceeding 26,000 ppm, while cadmium, molybdenum, and copper were also elevated. Detailed results for chromium, cadmium, molybdenum, and copper are presented in the following section.

PNR 2	Arsenic (As) (ppm)			Nickel (Ni) (ppm)		
	Min	Max	Average	Min	Max	Average
Stark	-	-	-	-	-	-
Hushpuckney	3	196	37	140	673	328
Mound City	4	33	10	132	619	253
Nuyaka Creek	5	437	68	83	573	314
Lake Neosho	2	3	2	173	534	253
Anna	4	30	12	26	553	243
Binkley	3	47	15	27	553	266

Excello	-	-	-	-	-	-
---------	---	---	---	---	---	---

Table 3. Data showing arsenic and nickel content (range and average) in the studied shales from the PNR 2 core, measured with pXRF.

PNR 2	Vanadium (V) (ppm)			Zinc (Zn) (ppm)		
	Min	Max	Average	Min	Max	Average
Stark	-	-	-	-	-	-
Hushpuckney	106	2,058	743	412	4,566	1,305
Mound City	72	2,128	395	205	20,756	1,392
Nuyaka Creek	77	1,437	605	88	13,377	1,502
Lake Neosho	120	758	353	243	1,593	555
Anna	75	1,119	262	12	5,003	332
Binkley	74	1,952	681	25	26,368	1,512
Excello	-	-	-	-	-	-

Table 4. Data showing vanadium and zinc content (range and average) in the studied shales from the PNR 2 core, measured with pXRF.

D.C.C 1 — Demonstrated widespread enrichment of arsenic, nickel, vanadium, and zinc throughout the Hushpuckney and Stark shales. Vanadium exceeded 3,000 ppm, zinc reached over 7,000 ppm, and arsenic values were consistently elevated. The Binkley and Nuyaka Creek shales also contained significant metal concentrations.

D.C.C 1	Arsenic (As) (ppm)			Nickel (Ni) (ppm)		
	Min	Max	Average	Min	Max	Average
Stark	8	44	25.5	79	718	386
Hushpuckney	11	67	28	56	608	283
Mound City	3	15	7	31	165	86
Nuyaka Creek	3	102	25.5	39	648	284
Lake Neosho	3	39	11	39	107	64
Anna	-	-	-	-	-	-
Binkley	3	98	20	54	917	385
Excello	2	11	4	15	373	190

Table 5. Data showing arsenic and nickel content (range and average) in the studied shales from the D.C.C 1 core, measured with pXRF.

D.C.C 1	Vanadium (V) (ppm)			Zinc (Zn) (ppm)		
	Min	Max	Average	Min	Max	Average
Stark	102	3,570	1,207	47	7,458	1,893
Hushpuckney	58	3,268	969	34	7,816	1,255
Mound City	73	298	170	22	154	72
Nuyaka Creek	163	2,137	973	32	6,827	1,299
Lake Neosho	61	133	209	19	87	52
Anna	-	-	-	-	-	-
Binkley	108	2,258	830	87	12,358	1,664
Excello	100	946	316	27	1,044	394

Table 6. Data showing vanadium and zinc content (range and average) in the studied shales from the D.C.C 1 core, measured with pXRF.

Edmonds 1-A — Displayed moderate enrichment across most shales, with localized peaks in the Anna and Hushpuckney shales. Vanadium concentrations reached 3,471 ppm, and zinc exceeded 15,000 ppm in the Anna shale. Arsenic and nickel were elevated primarily in the Stark and Hushpuckney shales.

Edmonds 1-A	Arsenic (As) (ppm)			Nickel (Ni) (ppm)		
	Min	Max	Average	Min	Max	Average
Stark	12	67	26	56	917	371
Hushpuckney	18	151	50	154	618	356
Mound City	3	28	10	65	210	118
Nuyaka Creek	2	66	18	50	372	210
Lake Neosho	2	5	3	130	290	186
Anna	5	53	21	110	730	457
Binkley	2	25	14	35	339	82
Excello	3	582	32	36	533	200

Table 7. Data showing arsenic and nickel content (range and average) in the studied shales from the Edmonds 1-A core, measured with pXRF.

Edmonds 1-A	Vanadium (V) (ppm)			Zinc (Zn) (ppm)		
	Min	Max	Average	Min	Max	Average
Stark	125	2,643	934	57	8,834	1,680
Hushpuckney	182	3,471	1,472	138	10,330	2,909
Mound City	76	694	246	69	392	178
Nuyaka Creek	195	994	546	26	1,722	657
Lake Neosho	169	1,205	396	203	2,197	582
Anna	138	1,480	632	122	15,964	1,648
Binkley	54	1,655	161	18	2,313	89
Excello	71	1,901	498	34	4,732	802

Table 8. Data showing vanadium and zinc content (range and average) in the studied shales from the Edmonds 1-A core, measured with pXRF.

Hinthorn CW-1 — Contained the strongest enrichment among all cores. The Stark and Hushpuckney shales averaged vanadium values above 1,000 ppm, while the Excello shale exhibited extreme zinc enrichment, with values exceeding 39,000 ppm. Arsenic reached 676 ppm in the Hushpuckney shale.

Hinthorn CW-1	Arsenic (As) (ppm)			Nickel (Ni) (ppm)		
	Min	Max	Average	Min	Max	Average
Stark	7	97	57	34	974	404
Hushpuckney	13	676	59	113	487	291
Mound City	3	43	13.5	44	419	182
Nuyaka Creek	4	115	24	46	451	235
Lake Neosho	3	102	25	77	1,687	448
Anna	2	68	7	13	129	49
Binkley	4	97	17	68	478	213
Excello	8	52	19	102	615	238

Table 9. Data showing arsenic and nickel content (range and average) in the studied shales from the Hinthorn CW-1 core, measured with pXRF.

Hinthon CW-1	Vanadium (V) (ppm)			Zinc (Zn) (ppm)		
	Min	Max	Average	Min	Max	Average
Stark	126	2,194	1,356	7	2,892	1,083
Hushpuckney	116	2,946	1,171	188	5,648	1,205
Mound City	92	1,122	247	129	2,556	514
Nuyaka Creek	65	1,416	572	33	5,427	530
Lake Neosho	97	1,023	269	236	32,758	1,407
Anna	64	1,185	214	8	253	46
Binkley	80	1,965	504	88	14,782	799
Excello	86	1,864	379	130	39,518	1,580

Table 10. Data showing vanadium and zinc content (range and average) in the studied shales from the Hinthon CW-1 core, measured with pXRF.

Tietjens 1-12 — Showed elevated metal concentrations consistent with regional trends. The Hushpuckney and Stark shales contained the highest vanadium (3,141 ppm) and zinc (6,745 ppm) concentrations, respectively, while arsenic and nickel were enriched in the Stark and Hushpuckney shales.

Tietjens 1-12	Arsenic (As) (ppm)			Nickel (Ni) (ppm)		
	Min	Max	Average	Min	Max	Average
Stark	15	68	30	68	907	352
Hushpuckney	12	60	29	141	688	431
Mound City	6	36	14	60	350	95
Nuyaka Creek	4	32	13	145	299	239
Lake Neosho	2	23	8	39	91	59
Anna	8	34	15	45	593	225
Binkley	2	46	11	48	851	181
Excello	3	65	13	20	646	210

Table 11. Data showing arsenic and nickel content (range and average) in the studied shales from the Tietjens 1-12 core, measured with pXRF.

Tietjens 1-12	Vanadium (V) (ppm)			Zinc (Zn) (ppm)		
	Min	Max	Average	Min	Max	Average
Stark	91	2,800	887	73	6,745	1,683
Hushpuckney	128	3,141	1,412	110	5,433	2,349
Mound City	65	537	138	71	1,018	169
Nuyaka Creek	584	2,055	1,021	469	1,852	1,126
Lake Neosho	66	159	112	58	92	75
Anna	68	1,108	375	20	3,555	784
Binkley	65	3,141	581	80	1,906	540
Excello	62	899	207	89	1,752	579

Table 12. Data showing vanadium and zinc content (range and average) in the studied shales from the Tietjens 1-12 core, measured with pXRF.

3.2 Concentrations of other important elements in Pennsylvanian black shales by pXRF

Concentrations of cadmium, chromium, copper, molybdenum, selenium, and uranium were variable across cores but generally highest in the Hushpuckney, Mound City, and Binkley shales.

Cadmium peaked at 456 ppm, chromium exceeded 1,600 ppm, and molybdenum reached over 200 ppm in localized zones. Selenium concentrations up to 300 ppm and uranium up to 549 ppm were measured in several shales, particularly within organic-rich intervals.

PNR 1 — Hushpuckney and Binkley had the highest averages for cadmium and chromium, exceeding 80 ppm and 400 ppm, respectively. Copper and molybdenum were also enriched, particularly in Hushpuckney shale. Selenium and uranium concentrations were highest in Hushpuckney and Binkley shales, with selenium reaching 300 ppm and uranium up to 549 ppm.

PNR 1	Cadmium (Cd) (ppm)			Chromium (Cr) (ppm)		
	Min	Max	Average	Min	Max	Average
Stark	-	-	-	-	-	-
Hushpuckney	13	252	83	177	1,169	596
Mound City	12	48	20	31	874	265
Nuyaka Creek	11	47	20	44	449	281
Lake Neosho	-	-	-	-	-	-
Anna	10	39	17	25	1,052	424
Binkley	11	290	57	24	1,057	450
Excello	11	63	24	25	1,488	331

Table 13. Data showing cadmium and chromium content (range and average) in the studied shales from the PNR 1 core, measured with pXRF.

PNR 1	Copper (Cu) (ppm)			Molybdenum (Mo) (ppm)		
	Min	Max	Average	Min	Max	Average
Stark	-	-	-	-	-	-
Hushpuckney	65	288	130	6	451	90
Mound City	13	112	50	3	51	8
Nuyaka Creek	18	144	84	7	122	32
Lake Neosho	-	-	-	-	-	-
Anna	44	332	124	3	158	20
Binkley	26	634	133	9	226	48
Excello	8	270	79	3	16	8

Table 14. Data showing copper and molybdenum content (range and average) in the studied shales from the PNR 1 core, measured with pXRF.

PNR 1	Lead (Pb) (ppm)			Rubidium (Rb) (ppm)		
	Min	Max	Average	Min	Max	Average
Stark	-	-	-	-	-	-
Hushpuckney	39	482	104	18	170	119
Mound City	18	194	43	78	198	142
Nuyaka Creek	34	198	118	12	188	108
Lake Neosho	-	-	-	-	-	-
Anna	26	166	69	38	158	123
Binkley	15	168	56	35	161	107
Excello	5	28	12	4	223	134

Table 15. Data showing lead and rubidium content (range and average) in the studied shales from the PNR 1 core, measured with pXRF.

PNR 1	Selenium (Se) (ppm)			Uranium (U) (ppm)		
	Min	Max	Average	Min	Max	Average
Stark	-	-	-	-	-	-
Hushpuckney	3	300	104	8	549	68
Mound City	2	34	14	3	72	14
Nuyaka Creek	4	51	32	10	167	37
Lake Neosho	-	-	-	-	-	-
Anna	2	119	39	5	142	19
Binkley	2	120	48	4	213	31
Excello	2	2	2	3	294	28

Table 16. Data showing selenium and uranium content (range and average) in the studied shales from the PNR 1 core, measured with pXRF.

PNR 2 — Cadmium and chromium values were higher than in PNR 1, especially in Hushpuckney and Mound City shales, with cadmium up to 383 ppm and chromium over 1,400 ppm. Copper concentrations reached over 600 ppm, while zinc and molybdenum were elevated in Hushpuckney and Binkley shales.

PNR 2	Cadmium (Cd) (ppm)			Chromium (Cr) (ppm)		
	Min	Max	Average	Min	Max	Average
Stark	-	-	-	-	-	-
Hushpuckney	11	383	41	64	1,423	621
Mound City	11	286	31	128	1,128	444
Nuyaka Creek	11	183	42	30	719	306
Lake Neosho	10	22	14	42	1,232	402
Anna	12	42	19	27	1,024	364
Binkley	11	266	53	26	1,019	384
Excello	-	-	-	-	-	-

Table 17. Data showing cadmium and chromium content (range and average) in the studied shales from the PNR 2 core, measured with pXRF.

PNR 2	Copper (Cu) (ppm)			Molybdenum (Mo) (ppm)		
	Min	Max	Average	Min	Max	Average
Stark	-	-	-	-	-	-
Hushpuckney	68	608	164	4	128	43
Mound City	52	250	99	2	149	22
Nuyaka Creek	26	244	95	4	94	33
Lake Neosho	7	19	12	5	5	5
Anna	9	299	95	3	127	20
Binkley	41	229	112	4	176	43
Excello	-	-	-	-	-	-

Table 18. Data showing copper and molybdenum content (range and average) in the studied shales from the PNR 2 core, measured with pXRF.

PNR 2	Lead (Pb) (ppm)			Rubidium (Rb) (ppm)		
	Min	Max	Average	Min	Max	Average
Stark	-	-	-	-	-	-
Hushpuckney	39	482	104	18	170	119
Mound City	18	194	43	78	198	142
Nuyaka Creek	34	198	118	12	188	108

Lake Neosho	26	166	69	38	158	123
Anna	15	168	56	35	161	107
Binkley	5	28	12	4	223	134
Excello	-	-	-	-	-	-

Table 19. Data showing lead and rubidium content (range and average) in the studied shales from the PNR 2 core, measured with pXRF.

PNR 2	Selenium (Se) (ppm)			Uranium (U) (ppm)		
	Min	Max	Average	Min	Max	Average
Stark	-	-	-	-	-	-
Hushpuckney	3	300	104	8	549	68
Mound City	2	34	14	3	72	14
Nuyaka Creek	4	51	32	10	167	37
Lake Neosho	2	119	39	5	142	19
Anna	2	120	48	4	213	31
Binkley	2	2	2	3	294	28
Excello	-	-	-	-	-	-

Table 20. Data showing selenium and uranium content (range and average) in the studied shales from the PNR 2 core, measured with pXRF.

D.C.C 1 — Hushpuckney and Nuyaka Creek shale members displayed high cadmium, chromium, and copper concentrations. Selenium ranged from 2 to 293 ppm, with uranium values as high as 345 ppm. The Binkley and Excello shale members consistently exhibited moderate enrichment across multiple trace elements.

D.C.C 1	Cadmium (Cd) (ppm)			Chromium (Cr) (ppm)		
	Min	Max	Average	Min	Max	Average
Stark	12	270	92	32	811	405
Hushpuckney	10	267	88	35	949	361
Mound City	11	19	14	24	691	178
Nuyaka Creek	11	237	76	60	515	283
Lake Neosho	11	24	16	22	68	37
Anna	-	-	-	-	-	-
Binkley	12	238	45	45	1,106	472
Excello	12	49	20	40	1,136	363

Table 21. Data showing cadmium and chromium content (range and average) in the studied shales from the D.C.C 1 core, measured with pXRF.

D.C.C 1	Copper (Cu) (ppm)			Molybdenum (Mo) (ppm)		
	Min	Max	Average	Min	Max	Average
Stark	31	187	112	5	733	188
Hushpuckney	32	217	105	4	633	103
Mound City	9	382	52	2	12	6
Nuyaka Creek	23	199	107	3	5,412	543
Lake Neosho	8	47	33	2	19	5
Anna	-	-	-	-	-	-
Binkley	38	931	174	2	375	60

Excello	7	45	15	2	7	4
---------	---	----	----	---	---	---

Table 22. Data showing copper and molybdenum content (range and average) in the studied shales from the D.C.C 1 core, measured with pXRF.

D.C.C 1	Lead (Pb) (ppm)			Rubidium (Rb) (ppm)		
	Min	Max	Average	Min	Max	Average
Stark	13	59	35	73	157	109
Hushpuckney	23	177	62	48	157	115
Mound City	13	126	34	63	181	120
Nuyaka Creek	31	526	134	24	162	116
Lake Neosho	9	88	35	111	197	170
Anna	-	-	-	-	-	-
Binkley	15	429	67	36	160	116
Excello	3	178	22	11	226	147

Table 23. Data showing lead and rubidium content (range and average) in the studied shales from the D.C.C 1 core, measured with pXRF.

D.C.C 1	Selenium (Se) (ppm)			Uranium (U) (ppm)		
	Min	Max	Average	Min	Max	Average
Stark	13	186	87	10	336	79
Hushpuckney	2	126	56	5	345	56
Mound City	1	69	21	4	96	17
Nuyaka Creek	11	293	74	8	245	48
Lake Neosho	2	2	2	3	9	5
Anna	-	-	-	-	-	-
Binkley	2	147	41	5	108	35
Excello	2	70	18	3	138	32

Table 24. Data showing selenium and uranium content (range and average) in the studied shales from the D.C.C 1 core, measured with pXRF.

Edmonds 1-A — Cadmium, and chromium reached peak values in the Anna and Hushpuckney shales. Molybdenum was highest in Stark and Hushpuckney shales, while selenium values up to 170 ppm were observed in Anna shale. Uranium enrichment was modest, averaging below 80 ppm across most members.

Edmonds 1-A	Cadmium (Cd) (ppm)			Chromium (Cr) (ppm)		
	Min	Max	Average	Min	Max	Average
Stark	11	164	70	118	951	473
Hushpuckney	11	287	107	212	856	544
Mound City	10	23	15	141	1,049	406
Nuyaka Creek	13	104	35	25	846	255
Lake Neosho	11	51	16	166	1,532	465
Anna	9	189	41	219	1,543	920
Binkley	11	54	16	62	1,048	124
Excello	10	160	36	36	1,985	625

Table 25. Data showing cadmium and chromium content (range and average) in the studied shales from the Edmonds 1-A core, measured with pXRF.

Edmonds 1-A	Copper (Cu) (ppm)			Molybdenum (Mo) (ppm)		
	Min	Max	Average	Min	Max	Average
Stark	19	228	105	11	778	196
Hushpuckney	49	173	124	25	719	230
Mound City	16	98	34	3	6	4
Nuyaka Creek	8	40	17	2	11	4
Lake Neosho	8	46	16	4	15	8
Anna	62	330	169	9	733	106
Binkley	9	238	38	4	230	29
Excello	12	464	126	4	523	46

Table 26. Data showing copper and molybdenum content (range and average) in the studied shales from the Edmonds 1-A core, measured with pXRF.

Edmonds 1-A	Lead (Pb) (ppm)			Rubidium (Rb) (ppm)		
	Min	Max	Average	Min	Max	Average
Stark	15	242	82	67	162	113
Hushpuckney	48	328	98	64	154	107
Mound City	5	34	14	74	176	128
Nuyaka Creek	4	317	50	73	202	143
Lake Neosho	5	39	12	85	185	156
Anna	39	497	152	45	155	102
Binkley	10	215	49	56	160	106
Excello	3	1,305	98	8	168	91

Table 27. Data showing lead and rubidium content (range and average) in the studied shales from the Edmonds 1-A core, measured with pXRF.

Edmonds 1-A	Selenium (Se) (ppm)			Uranium (U) (ppm)		
	Min	Max	Average	Min	Max	Average
Stark	13	138	60	8	365	76
Hushpuckney	16	141	64	7	282	78
Mound City	2	8	4	8	135	40
Nuyaka Creek	3	44	12	6	83	32
Lake Neosho	2	12	5	4	153	19
Anna	7	170	65	7	232	41
Binkley	2	86	9	3	104	9
Excello	2	542	60	3	512	43

Table 28. Data showing selenium and uranium content (range and average) in the studied shales from the Edmonds 1-A core, measured with pXRF.

Hinthorn CW-1 — Hushpuckney and Stark shales showed elevated levels for most trace elements.

Cadmium peaked at 456 ppm, chromium exceeded 1,600 ppm, and copper was above 250 ppm in several horizons. Selenium and uranium concentrations were widespread, averaging 40–100 ppm and 20–80 ppm respectively.

Hinthorn CW-1	Cadmium (Cd) (ppm)			Chromium (Cr) (ppm)		
	Min	Max	Average	Min	Max	Average
Stark	13	69	37	96	956	550
Hushpuckney	11	262	62	201	1,694	909
Mound City	11	49	19	32	1,000	257
Nuyaka Creek	11	90	28	80	775	352
Lake Neosho	10	456	36	126	744	431
Anna	12	26	17	53	490	121
Binkley	10	195	42	101	1,278	441
Excello	10	496	52	109	1,275	423

Table 29. Data showing cadmium and chromium content (range and average) in the studied shales from the Hinthorn CW-1 core, measured with pXRF.

Hinthorn CW-1	Copper (Cu) (ppm)			Molybdenum (Mo) (ppm)		
	Min	Max	Average	Min	Max	Average
Stark	11	146	84	12	296	115
Hushpuckney	24	250	111	11	4,030	161
Mound City	29	178	68	3	68	10
Nuyaka Creek	22	197	77	4	114	31
Lake Neosho	38	313	159	3	52	16
Anna	8	295	44	3	6	4
Binkley	33	185	101	3	350	41
Excello	27	1,469	145	5	363	45

Table 30. Data showing copper and molybdenum content (range and average) in the studied shales from the Hinthorn CW-1 core, measured with pXRF.

Hinthorn CW-1	Lead (Pb) (ppm)			Rubidium (Rb) (ppm)		
	Min	Max	Average	Min	Max	Average
Stark	47	319	149	18	151	123
Hushpuckney	11	595	75	33	162	113
Mound City	10	94	39	69	194	147
Nuyaka Creek	15	460	72	19	188	120
Lake Neosho	16	444	96	39	191	154
Anna	5	483	35	8	173	98
Binkley	20	207	49	58	165	121
Excello	10	65	22	12	151	101

Table 31. Data showing lead and rubidium content (range and average) in the studied shales from the Hinthorn CW-1 core, measured with pXRF.

Hinthorn CW-1	Selenium (Se) (ppm)			Uranium (U) (ppm)		
	Min	Max	Average	Min	Max	Average
Stark	10	92	62	17	178	84
Hushpuckney	10	530	101	5	140	37
Mound City	2	80	26	3	55	9
Nuyaka Creek	2	183	41	4	261	41
Lake Neosho	3	171	51	9	210	35
Anna	6	145	45	8	32	19
Binkley	2	137	50	3	102	18
Excello	2	174	52	3	164	22

Table 32. Data showing selenium and uranium content (range and average) in the studied shales from the Hinthorn CW-1 core, measured with pXRF.

Tietjens 1-12 — This core displayed balanced but consistent enrichment across metals. Cadmium reached 244 ppm and chromium exceeded 1,100 ppm. Selenium and uranium concentrations were generally moderate, with the Stark and Hushpuckney shale members showing the highest averages.

Tietjens 1-12	Cadmium (Cd) (ppm)			Chromium (Cr) (ppm)		
	Min	Max	Average	Min	Max	Average
Stark	11	244	84	99	1,146	471
Hushpuckney	13	236	106	241	889	553
Mound City	12	72	21	26	697	118
Nuyaka Creek	12	18	15	170	822	384
Lake Neosho	10	23	14	24	90	40
Anna	11	128	32	26	1,265	548
Binkley	12	56	24	34	1,130	384
Excello	11	38	18	59	706	383

Table 33. Data showing cadmium and chromium content (range and average) in the studied shales from the Tietjens 1-12 core, measured with pXRF.

Tietjens 1-12	Copper (Cu) (ppm)			Molybdenum (Mo) (ppm)		
	Min	Max	Average	Min	Max	Average
Stark	32	177	100	13	908	198
Hushpuckney	61	177	113	23	490	216
Mound City	17	113	35	3	78	15
Nuyaka Creek	9	673	123	4	116	29
Lake Neosho	6	274	28	3	3	3
Anna	29	232	121	5	228	47
Binkley	24	576	139	3	56	9
Excello	25	261	159	3	114	22

Table 34. Data showing copper and molybdenum content (range and average) in the studied shales from the Tietjens 1-12 core, measured with pXRF.

Tietjens 1-12	Lead (Pb) (ppm)			Rubidium (Rb) (ppm)		
	Min	Max	Average	Min	Max	Average
Stark	4	72	20	63	141	106
Hushpuckney	10	237	45	57	141	98
Mound City	21	641	63	61	141	120
Nuyaka Creek	12	172	48	114	182	154
Lake Neosho	6	117	16	113	174	149
Anna	16	56	31	33	153	105
Binkley	3	85	17	55	172	122
Excello	8	165	35	6	141	97

Table 35. Data showing lead and rubidium content (range and average) in the studied shales from the Tietjens 1-12 core, measured with pXRF.

Tietjens 1-12	Selenium (Se) (ppm)			Uranium (U) (ppm)		
	Min	Max	Average	Min	Max	Average
Stark	5	140	68	6	271	65
Hushpuckney	22	124	67	11	248	79

Mound City	2	45	11	6	218	23
Nuyaka Creek	2	30	11	31	88	51
Lake Neosho	1	44	9	3	13	8
Anna	1	145	65	4	98	26
Binkley	2	66	16	4	145	36
Excello	5	353	41	8	94	36

Table 36. Data showing selenium and uranium content (range and average) in the studied shales from the Tietjens 1-12 core, measured with pXRF.

3.3 Other results

3.3.1 Geochemistry results of RSE

The ICP-OES/MS results show that the Stark and Hushpuckney units contain the greatest enrichment of redox-sensitive elements (RSE) concentration. The average results for the six cores are presented in tables 37 and 38. Additional data for other shale members are attached and will be available for each state survey on the [Earth MRI Black Shales project page](#) on the KGS website.

Stark Shale Member

Core	Mo	V	Ni	Zn	Cd	U	Pb
	Average	Average	Average	Average	Average	Average	Average
PNR 1	-	-	-	-	-	-	-
PNR 2	-	-	-	-	-	-	-
D.C.C 1	117	904	366	1,536	42	76	44
Hinthorn CW-1	161	1,858	415	2,562	66	121	440
Edmonds 1-A	315	1,610	403	3,218	1,657	130	196
Tietjens 1-12	275	1,487	391	2,579	106	97	30

Table 37. Average concentration of RSEs analyses in ppm.

Hushpuckney Shale Member

Core	Mo	V	Ni	Zn	Cd	U	Pb
	Average	Average	Average	Average	Average	Average	Average
PNR 1	203	1,672	343	2,563	94	85	133
PNR 2	124	1,515	356	2,461	84	131	52
D.C.C 1	257	1,646	344	2,004	162	96	119
Hinthorn CW-1	252	1,548	310	1,471	48	58	100
Edmonds 1-A	289	2,091	366	4,408	138	125	222
Tietjens 1-12	440	3,019	446	3,974	178	174	138

Table 38. Average concentration of RSEs analyses in ppm.

3.3.2 Total organic carbon and sulfur contents

Total organic carbon (TOC) values ranged from below 1 wt% to over 30 wt%, with the highest concentrations in the Anna, Hushpuckney, and Nuyaka Creek shales. The Anna shale exhibited TOC

averages exceeding 16 wt%, while the Nuyaka Creek shale averaged 13 wt%. Sulfur values were moderate, typically ranging from 0.5 to 3 wt%, but locally exceeded 6 wt% in the Nuyaka Creek shale of PNR 1. The Excello shale generally had the lowest TOC and sulfur concentrations in all cores. Organic carbon and sulfur data reveal a strong variation across shale members and three examined subsurface cores.

PNR 1 — TOC values ranged from 0.1 to 32 wt%, with the highest averages in Anna shale (16.03%) and Nuyaka Creek shale (12.94%). Sulfur content was moderate, typically between 1 and 3 wt%, with maximums up to nearly 6.4 wt%.

PNR 1	TOC (wt. %)			Total sulfur (wt. %)		
	Min	Max	Average	Min	Max	Average
Stark	-	-	-	-	-	-
Hushpuckney	11.2	22.9	17.04	1.25	2.96	2.04
Mound City	1.18	12.34	5.49	0.46	1.98	1.1
Nuyaka Creek	1.82	19.7	12.94	0.98	6.38	3.18
Lake Neosho	-	-	-	-	-	-
Anna	5.37	32.03	16.03	0.92	4.88	2.01
Binkley	5	21.69	14.63	0.97	1.91	1.39
Excello	0.1	1.04	0.47	0	1.52	0.54

Table 39. Data table showing the total organic carbon (TOC) and total sulfur content (ranges and average values, uncertainty ± 0.01 for C and S) in PNR 1 shales.

PNR 2 — Hushpuckney, Nuyaka Creek, and Binkley shale members showed the highest organic carbon content, averaging 11–16 wt%, while sulfur content ranged between 0.4 and 2 wt%. Excello shale had low organic matter, averaging below 1 wt%.

PNR 2	TOC (wt. %)			Total sulfur (wt. %)		
	Min	Max	Average	Min	Max	Average
Stark	-	-	-	-	-	-
Hushpuckney	0.76	25.3	11.29	0.03	0.93	0.41
Mound City	4.38	21.06	9.47	0.9	2.03	1.33
Nuyaka Creek	0.02	39.48	16.45	0.02	3.16	1.99
Lake Neosho	-	-	-	-	-	-
Anna	0.02	25.48	10.85	1.07	1.84	1.42
Binkley	0.84	24.6	11.43	0.69	3.17	1.73
Excello	0.05	0.69	0.48	0.29	0.83	0.57

Table 40. Data table showing the total organic carbon (TOC) and total sulfur content (ranges and average values, uncertainty ± 0.01 for C and S) in PNR 2 shales.

D.C.C 1 — Hushpuckney, Anna, Binkley, and Nuyaka Creek shale members contained the highest TOC values (14–16 wt%), with sulfur contents averaging 1–2 wt%. Excello was again low in both carbon and sulfur.

Overall, the TOC and sulfur data indicate that the most organic-rich and sulfur-bearing shales correspond to the same members that exhibit the highest metal enrichments, suggesting strong geochemical association between organic matter and trace element accumulation.

D.C.C 1	TOC (wt. %)			Total sulfur (wt. %)		
	Min	Max	Average	Min	Max	Average
Stark	-	-	-	-	-	-
Hushpuckney	5.16	19.21	14.53	0.75	2.93	1.78
Mound City	0.25	0.84	0.61	0.65	1.49	1.11
Nuyaka Creek	1.37	31.11	16.47	0.72	2.75	1.66
Lake Neosho	-	-	-	-	-	-
Anna	1.31	21.13	14.97	0.6	2.41	1.58
Binkley	5.77	28.38	16.39	0.22	1.97	1.09
Excello	0.37	1.65	0.9	0	0.38	0.13

Table 41. Data table showing the total organic carbon (TOC) and total sulfur content (ranges and average values, uncertainty ± 0.02 for C and ± 0.04 for S) in D.C.C 1 shales.

3.3.3 X-ray Diffraction (XRD)

X-ray diffraction analyses of bulk samples and clay fraction samples were performed on multiple cores taken from several shale members. The resulting mineralogical data for clay fraction from the Hinthorn, Douglas County, and Edmonds intervals are summarized in the sections below.

Core	Shale Member	Depth (ft)	Chlorite (wt%)	Illite/Smectite (wt%)	Kaolinite (wt%)	Mica (wt%)	Quartz (wt%)
D.C.C 1	Anna	816.2	7	22	13	37	21
	Stark	549.3	24	10	0	30	36
Edmonds 1-A	Anna	659	16.8	10.9	16.8	30.7	16.8
	Excello	772.8	6.5	29	0	39.8	24.7
Hinthorn CW-1	Lake Neosho	389.7	25.7	26.7	0	26.7	20.8

Table 42. Mineralogy of the < 2-micron clay size fraction. Reported error is ± 5.0 %. All samples were subjected to air dried, glycolated, and heated treatments.

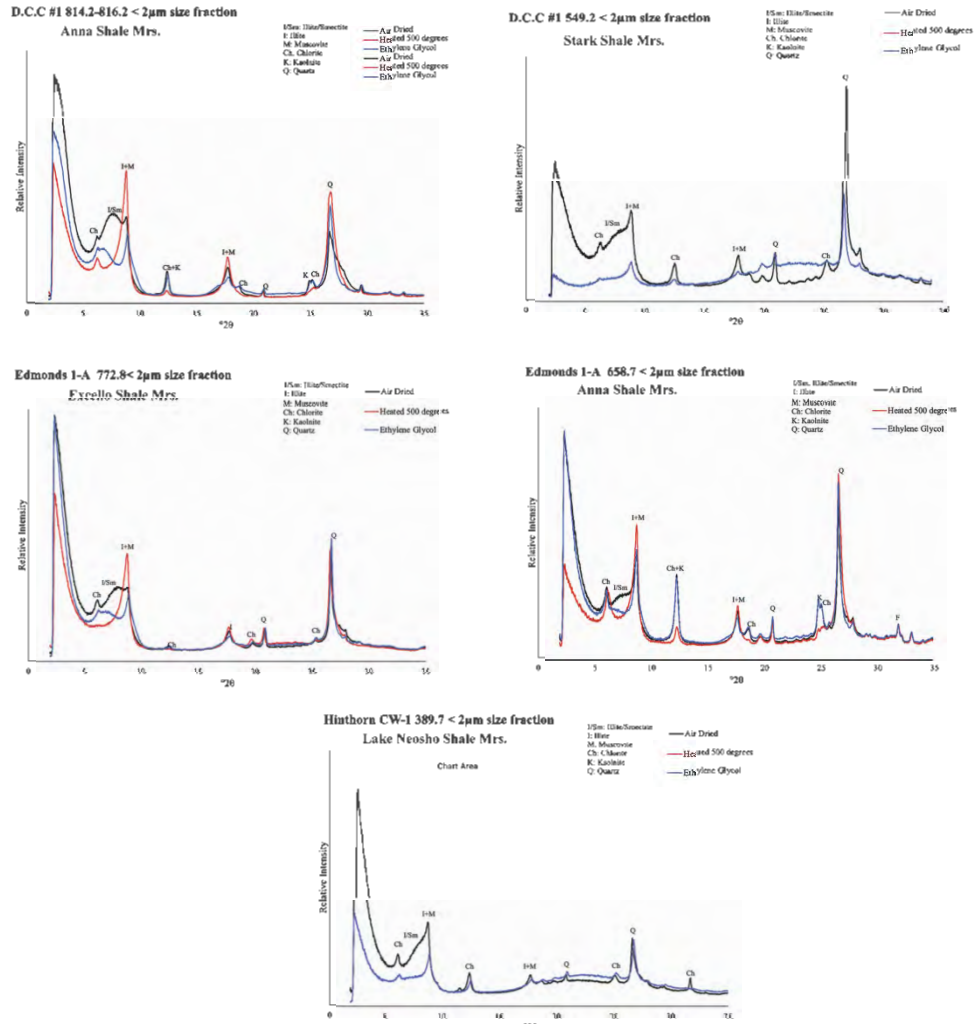


Figure 3. XRD analysis charts from clay size fraction collected from core D.C.C 1, Edmonds 1-A, and Hinthorn CW-1.

3.3.4 Scanning Electron Microscopy and Energy Dispersive Spectroscopy (SEM-EDS)

Figures 4–9 show EDS analysis results for some of the shale members.

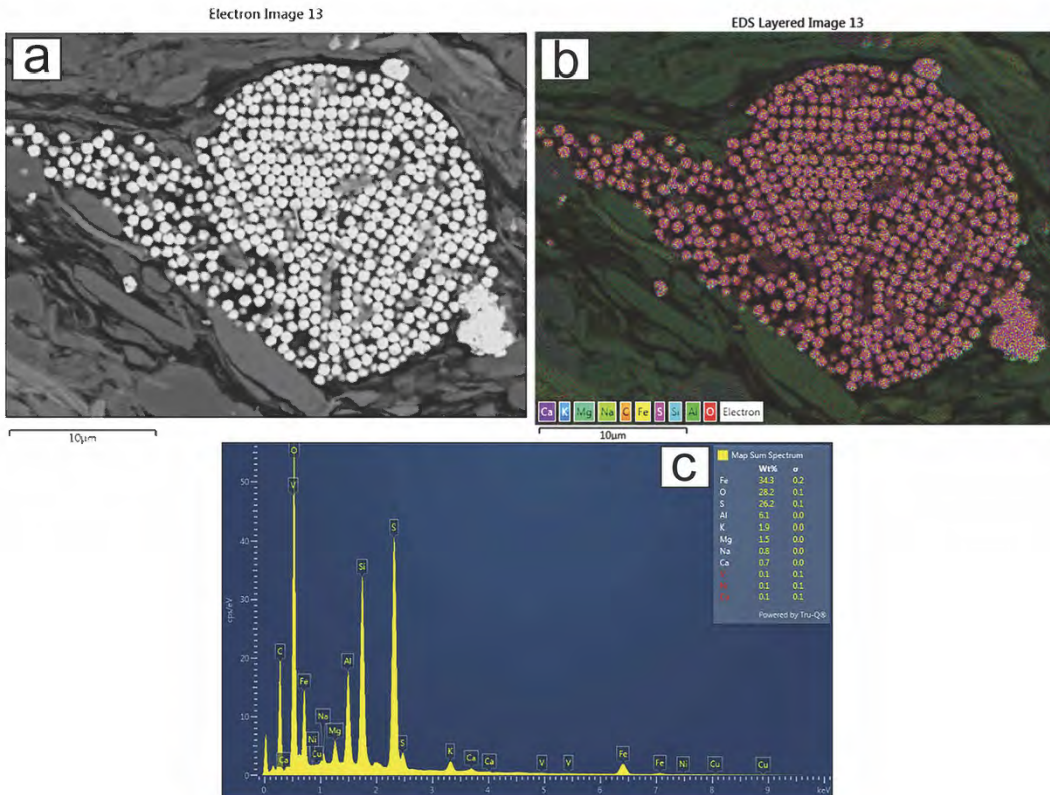


Figure 4. a) shows an electron image of a spherical particle cluster within the Hushpuckney shale from Hinthorn core site 1, b) shows the corresponding EDS layered map highlighting elemental distributions across the same field of view, and c) presents the EDS spectrum identifying the primary elemental components observed in the analysis.

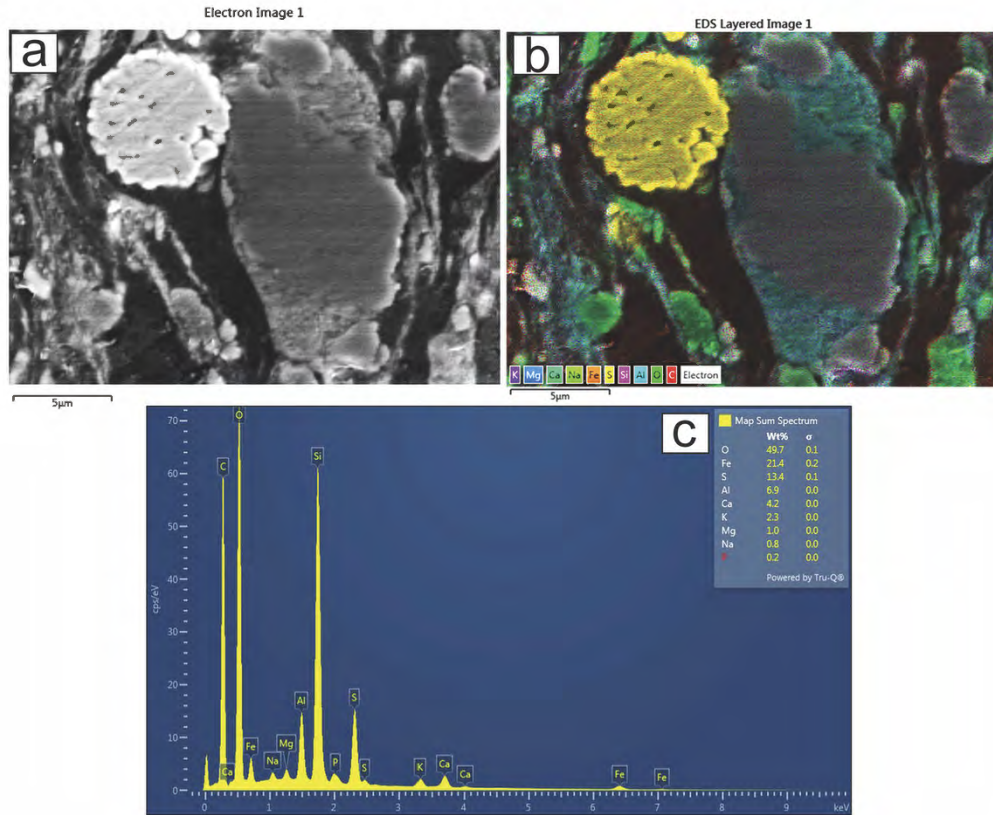


Figure 5. a) shows an electron image of particles within the Binkley shale from Hinthorn core site 1, b) shows the corresponding EDS layered map highlighting elemental distributions across the same field of view, and c) presents the EDS spectrum identifying the primary elemental components observed in the analysis.

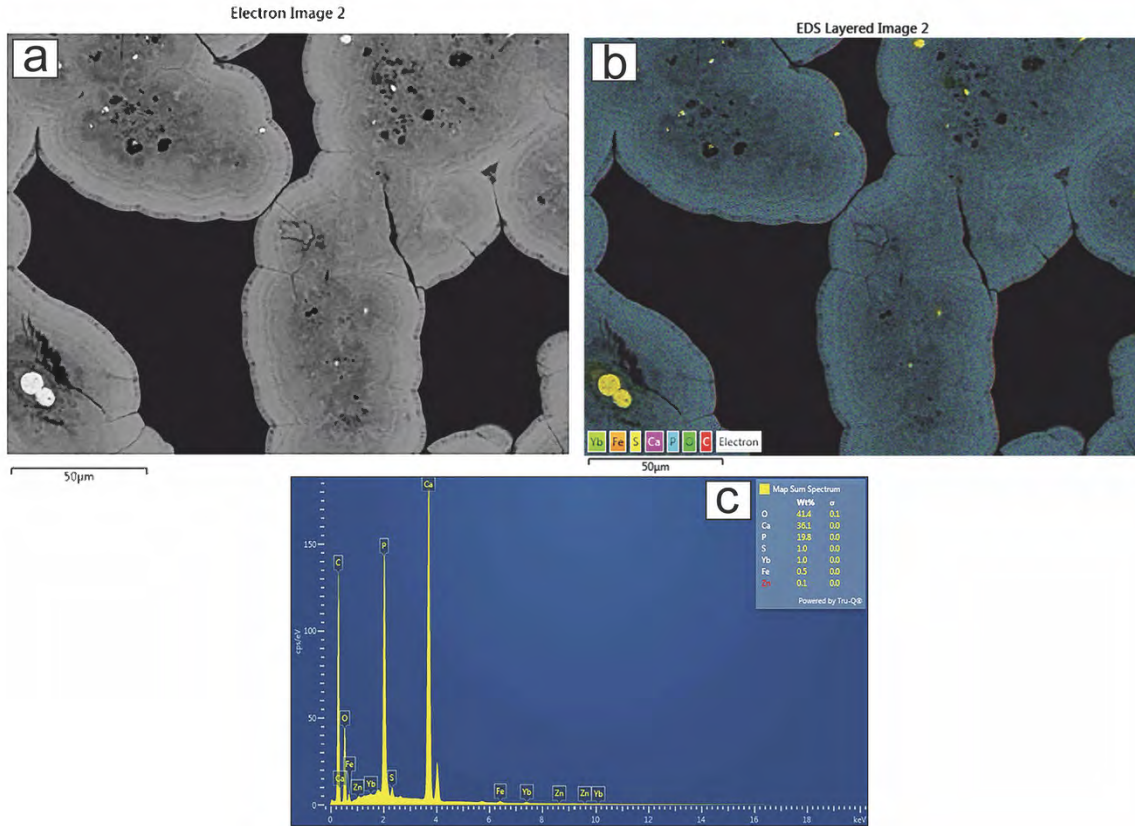


Figure 6. a) shows an electron image of phosphate nodules within the Hushpuckney shale from Hinthorn core site 5, b) shows the corresponding EDS layered map highlighting elemental distributions across the same field of view, and c) presents the EDS spectrum identifying the primary elemental components observed in the analysis.

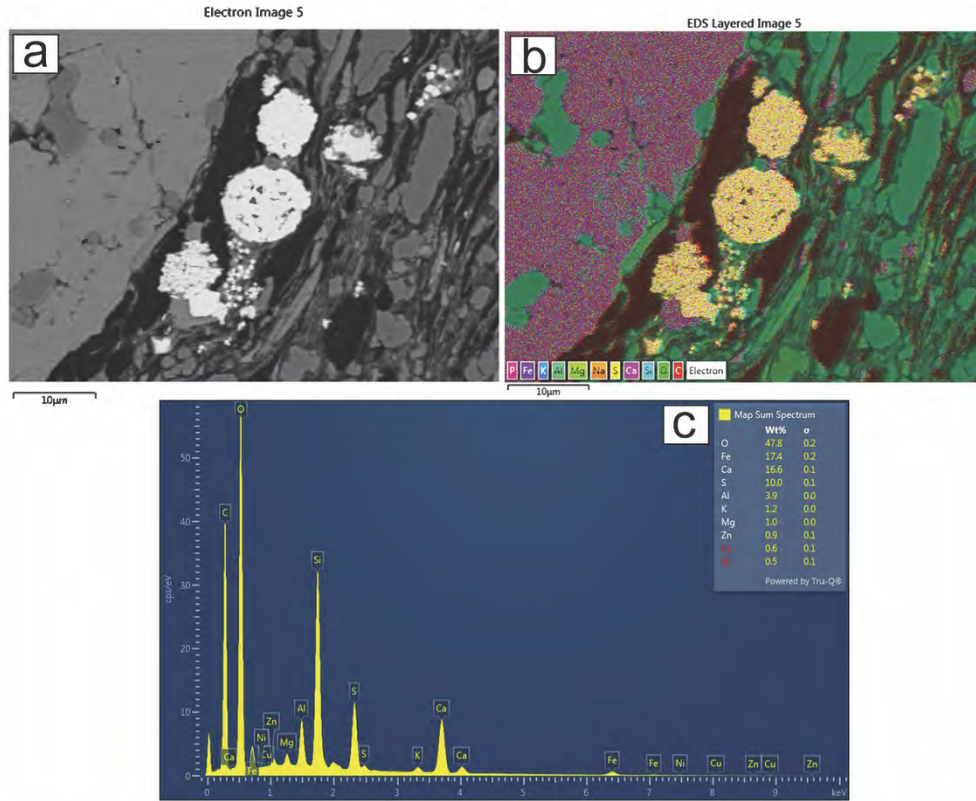


Figure 7. a) shows an electron image of particles within the Binkley shale from Hinthorn core site 5, b) shows the corresponding EDS layered map highlighting elemental distributions across the same field of view, and c) presents the EDS spectrum identifying the primary elemental components observed in the analysis.

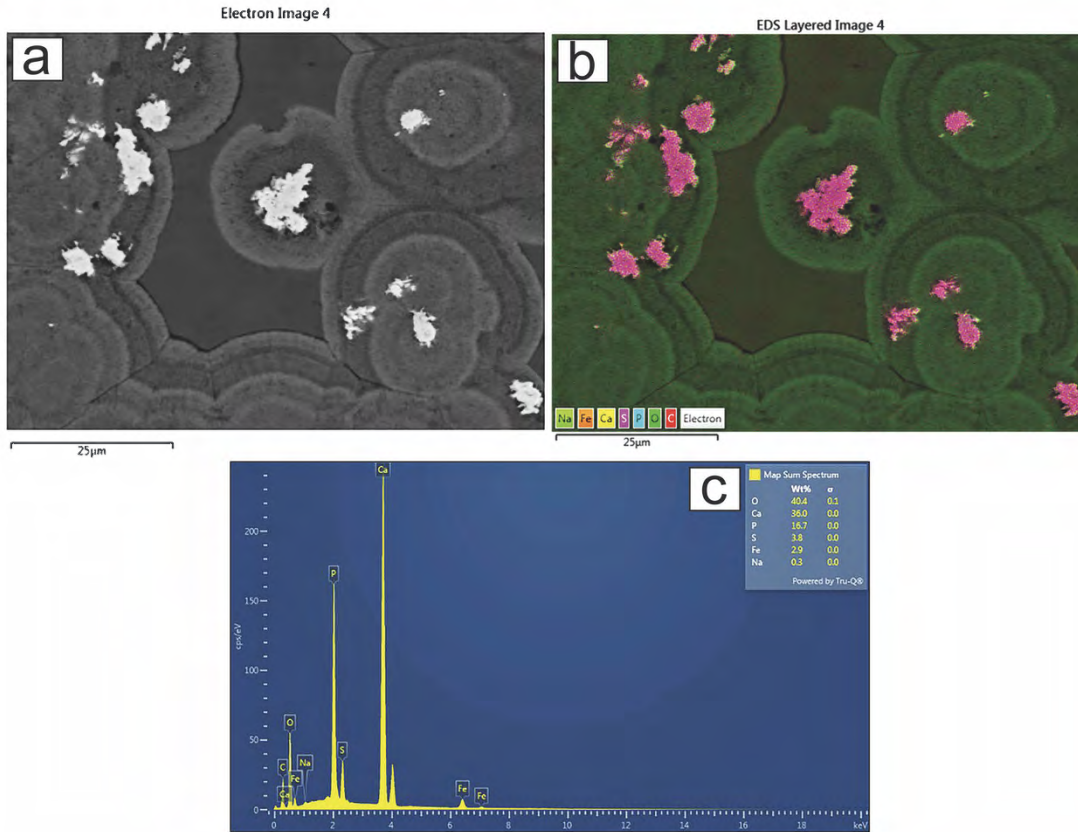


Figure 8. a) shows an electron image of phosphate nodules within the Hushpuckney shale from Hinthorn core site 7, b) shows the corresponding EDS layered map highlighting elemental distributions across the same field of view, and c) presents the EDS spectrum identifying the primary elemental components observed in the analysis.

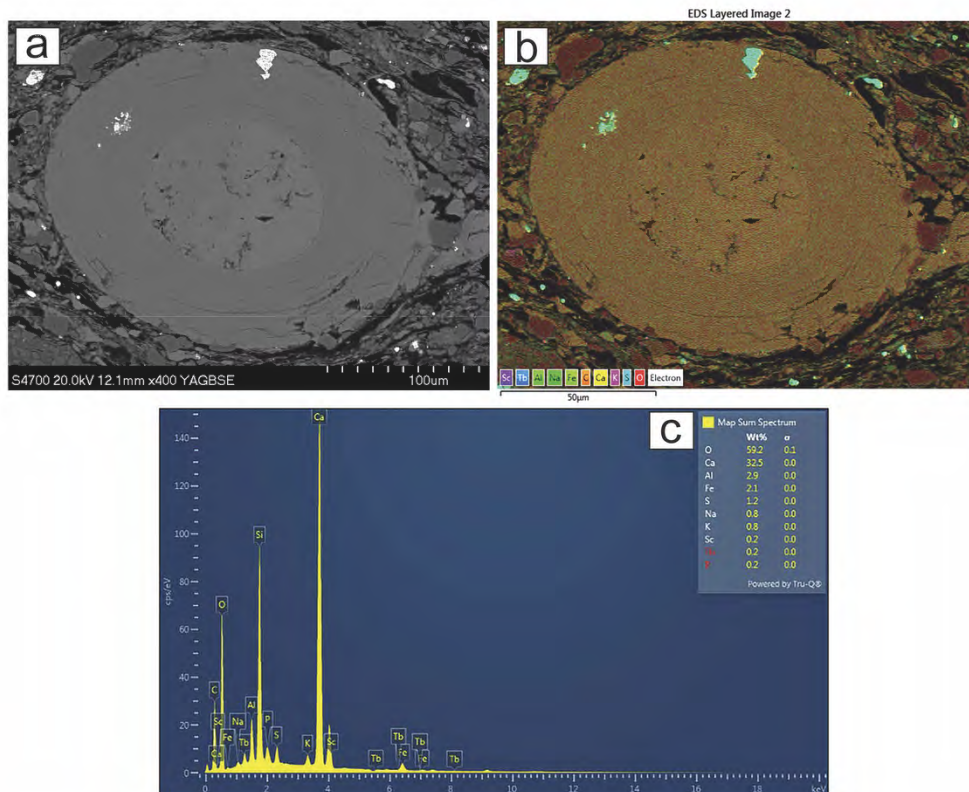


Figure 9. a) shows an BSE image of a phosphate nodule within the Binkley shale from Edmonds core, b) shows the corresponding EDS layered map that highlights elemental distributions across the same field of view, and c) presents the EDS spectrum identifying the primary elemental components observed in the analysis.

4. Discussion

4.1 Relative critical minerals enrichment of different shales (temporal comparison)

The combined pXRF and ICP datasets show that enrichment of critical minerals varies predictably among the examined Pennsylvanian shale members. Across all cores, the Stark and Hushpuckney shales consistently contain the highest concentrations of redox-sensitive elements, including vanadium, nickel, molybdenum, zinc, cadmium, and uranium. The Stark shale exhibits strong enrichment in several cores, such as D.C.C 1, Hinthorn CW-1, Edmonds 1-A, and Tietjens 1-12. The Hushpuckney shale shows equally strong and often higher enrichment in both major and trace elements, with zinc and cadmium reaching some of the highest values in the dataset. These trends are also reproduced in ICP analyses, which show elevated molybdenum, vanadium, and zinc in these same units.

The temporal pattern in enrichment corresponds to intervals of enhanced organic matter accumulation and bottom water restriction. Shales deposited during these intervals record some of the highest TOC values measured, as found in the Anna, Hushpuckney, and Nuyaka Creek members. The co-

occurrence of elevated TOC, sulfur content, and enriched trace metals indicates that depositional settings with suboxic to anoxic conditions played a dominant role in concentrating critical elements. The observation that the Excello shale consistently contains the lowest TOC values and correspondingly low metal concentrations further supports this temporal association between reducing conditions and enrichment. These relationships align with conceptual models for redox-driven trace metal sequestration in Pennsylvanian black shales.

4.2 Spatial distribution (maps) of elemental enrichment based on ICP OES and ICP MS data

Spatial variation in critical mineral enrichment among the sampled cores is evident in the ICP datasets, even though the analyzed shale members share a similar stratigraphic framework. The Hinthorn CW-1, Edmonds 1-A, D.C.C 1, and Tietjens 1-12 cores show consistently higher ICP reported concentrations of key redox-sensitive elements, particularly in the Stark and Hushpuckney shale members. For example, the Stark shale in Hinthorn CW-1 contains average ICP values of 161 ppm molybdenum, 1,858 ppm vanadium, and 415 ppm nickel, while Edmonds 1-A exhibits similarly elevated molybdenum and zinc averages in both the Stark and Hushpuckney shale members (tables 37 and 38). These values exceed those recorded in the other sampled cores and indicate that the depositional environment at these locations promoted more efficient preservation or concentration of redox-sensitive elements.

Intermediate enrichment characterizes the D.C.C 1 and PNR 2 cores. Both contain Stark and Hushpuckney units with elevated ICP averages relative to crustal background levels, although their concentrations do not reach the higher values observed in Hinthorn CW-1 or Edmonds 1-A. In contrast, enrichment patterns in PNR 1 are less pronounced, which suggests that conditions in this part of the basin were comparatively less reducing or less favorable for trace metal fixation during deposition and early diagenesis.

These spatial differences imply that the Cherokee-Forest City Basin contained multiple depositional subenvironments with varying degrees of water column restriction, organic matter preservation, and redox intensity. The higher ICP metal concentrations in cores such as Hinthorn CW-1, Edmonds 1-A, and Tietjens 1-12 are consistent with more reducing or more isolated depositional settings, whereas the lower values in PNR 1 point to comparatively better circulation or less restricted conditions. Overall, the ICP data indicate that spatial heterogeneity in redox conditions strongly influenced both the magnitude and distribution of critical mineral enrichment across the study area.

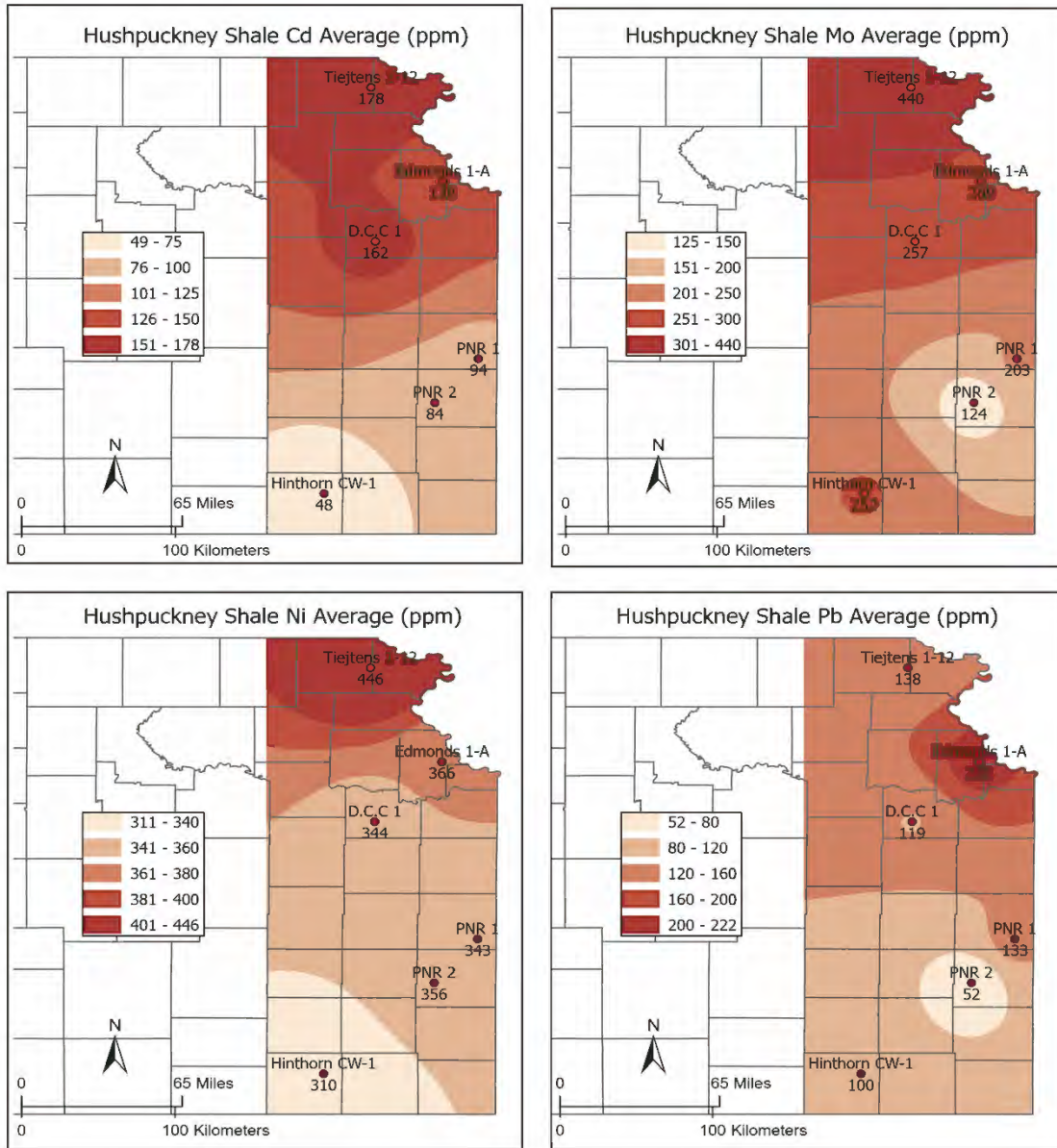


Figure 10. Distribution of cadmium (Cd), molybdenum (Mo), nickel (Ni), and lead (Pb) content (in ppm) in the Hushpuckney shale member in eastern Kansas. Values represent averages calculated from the samples analyzed in individual locations.

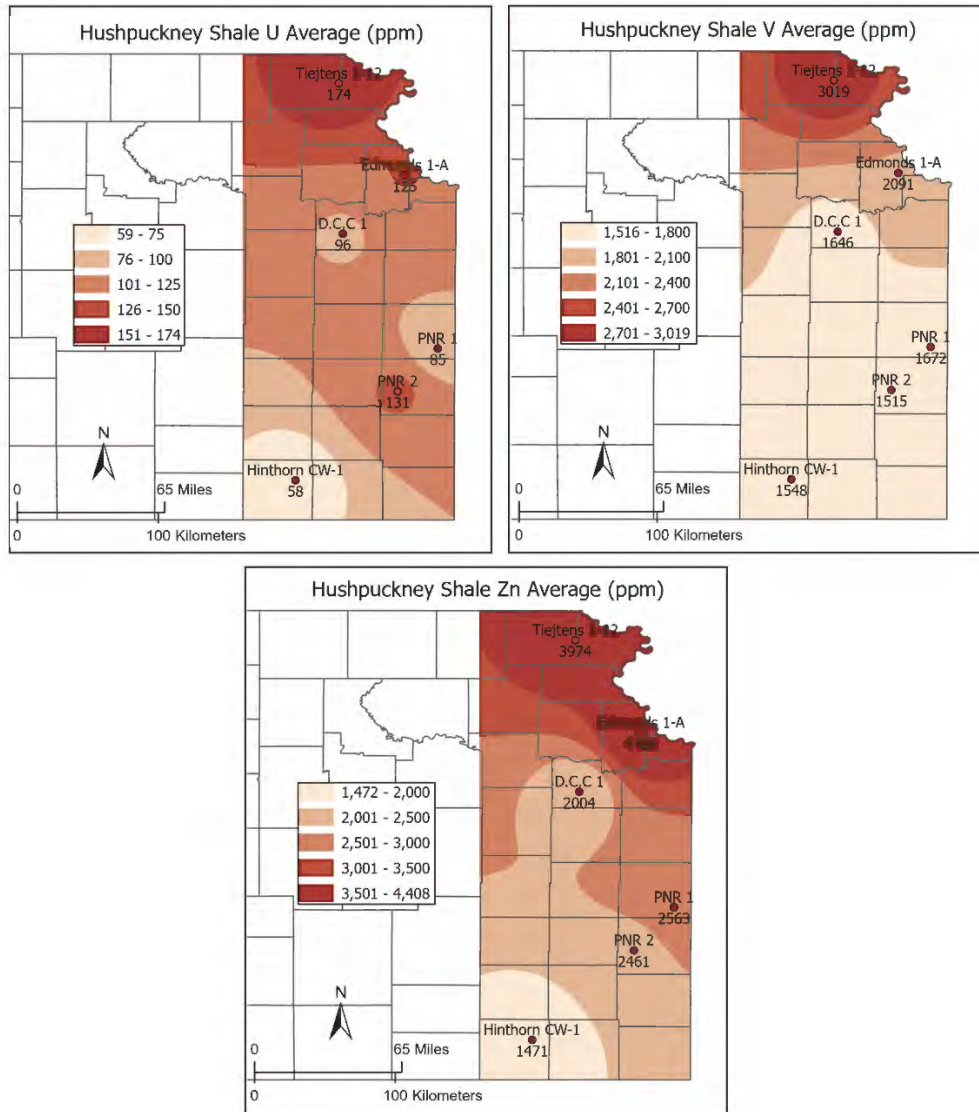


Figure 11. Distribution of uranium (U), vanadium (V), and zinc (Zn) content (in ppm) in the Hushpuckney shale member in eastern Kansas. Values represent averages calculated from the samples analyzed in individual locations.

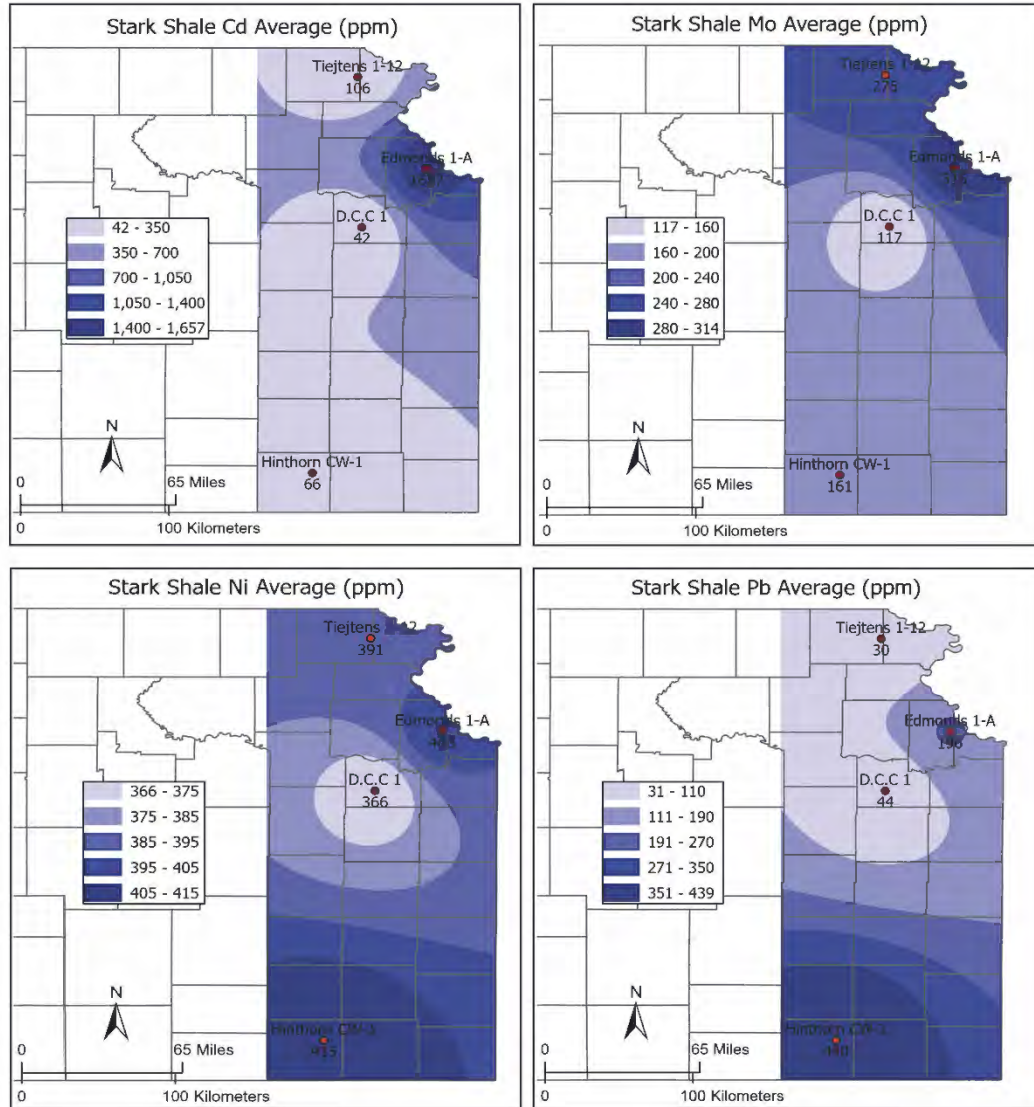


Figure 12. Distribution of cadmium (Cd), molybdenum (Mo), nickel (Ni), and lead (Pb) content (in ppm) in the Stark shale member in eastern Kansas. Values represent averages calculated from the samples analyzed in individual locations.

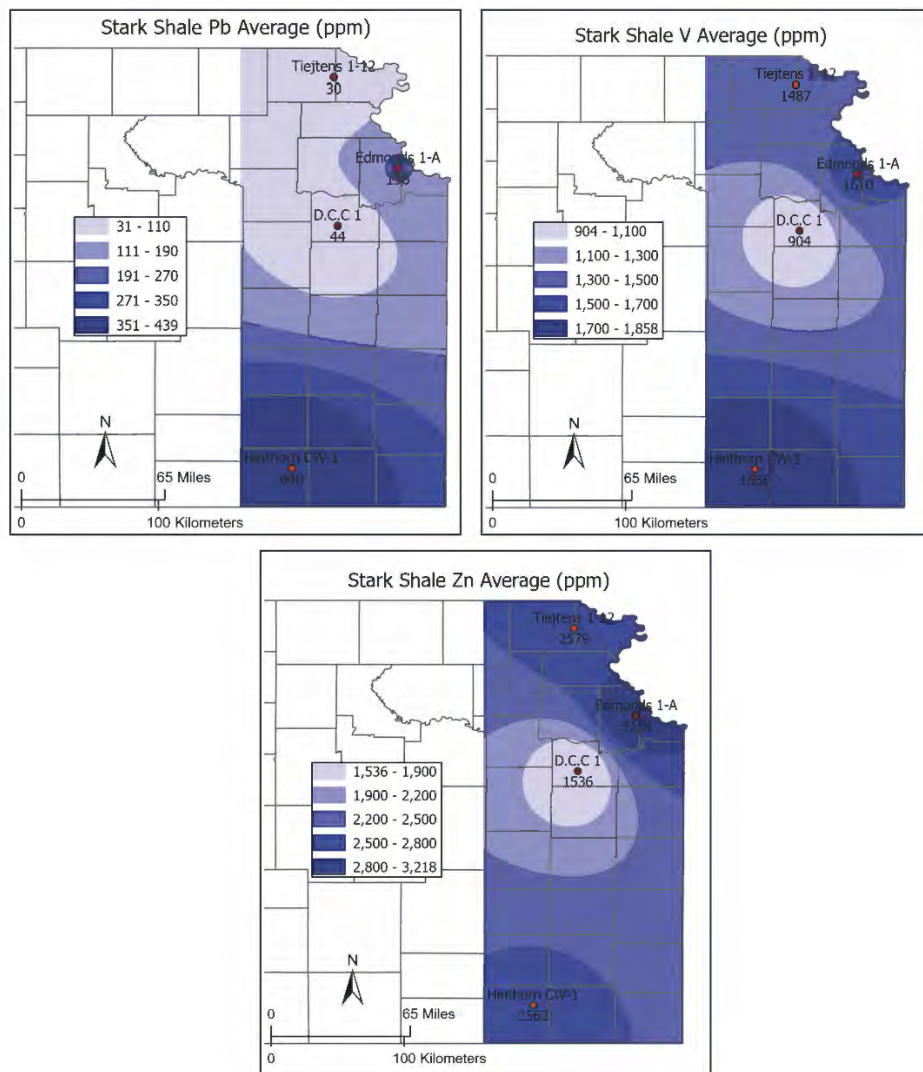


Figure 13. Distribution of uranium (U), vanadium (V), and zinc (Zn) content (in ppm) in the Stark shale member in eastern Kansas. Values represent averages calculated from the samples analyzed in individual locations.

4.3 Patterns associated with other results (TOC, S, P, etc.)

The relationship between trace metal concentrations and organic geochemical parameters is strong across the dataset. Shales with the highest TOC values also display some of the greatest enrichments in vanadium, nickel, molybdenum, and zinc. The Hushpuckney and Nuyaka Creek shales show both elevated TOC and substantial concentrations of redox-sensitive elements, indicating deposition during intervals with efficient preservation of organic matter. Elevated sulfur contents in these same units suggest active sulfate reduction, which would promote formation of pyrite and other metal-bearing sulfide phases. For example, sulfur values close to 6.4% in the Nuyaka Creek shale at PNR 1 (table 39) coincide

with high concentrations of vanadium, molybdenum, and cadmium. This pattern indicates that metal enrichment was mediated by sulfur-rich diagenetic pathways and early stabilization into sulfide minerals.

Mineralogical analyses further support this association. XRD results (table 40; fig. 3) show variable proportions of clay minerals, quartz, and apatite, and the presence of fluorapatite and phosphate nodules in some units is consistent with enhanced metal accumulation. SEM-EDS and back-scattered electrons (BES) imaging (e.g., figs. 4–9) demonstrate that metals occur within fine-grained pore-filling phases, disseminated sulfides, and phosphate-rich particles. The identification of these mineralogical hosts confirms that both organic matter and early diagenetic minerals played significant roles in trace metal sequestration. Units with greater apatite content also show higher concentrations of rare earth elements, indicating that phosphate phases served as additional reservoirs for critical elements.

4.4 Implications for critical mineral potential

The regional consistency of enriched shale members, combined with measurable spatial variability, demonstrates that Pennsylvanian black shales of eastern Kansas contain significant potential as repositories of critical minerals. In particular, the Stark and Hushpuckney shales show metal concentrations that exceed typical crustal averages by orders of magnitude and do so across multiple counties and core locations. The presence of localized extreme zinc values in the Excello shale at Hinthorn CW-1 (table 10) highlights the possibility of focused mineralization where basin conditions were most favorable. The integration of geochemical, mineralogical, and organic geochemical data indicates that enrichment was controlled primarily by depositional redox conditions and early diagenetic incorporation into sulfide and phosphate minerals rather than by detrital contributions. As a result, these shales represent laterally extensive and reliably predictable targets for future evaluation of vanadium, nickel, zinc, and molybdenum resources.

5. Conclusions

The ICP-based geochemical results demonstrate that Pennsylvanian black shales in eastern Kansas contain significant enrichment in several critical minerals, particularly in the Stark and Hushpuckney shale members. These units consistently show the highest concentrations of molybdenum, vanadium, nickel, zinc, cadmium, and lead among the measured intervals. The magnitude of enrichment, which is reproduced across multiple cores, confirms that these shales represent regionally extensive horizons of elevated critical mineral content within the Cherokee-Forest City Basin.

A clearer pattern emerges when comparing shale members across all cores. The Hushpuckney shale is the only unit that shows consistently high enrichment in every core and for most of the major

redox-sensitive elements. The Stark shale shows strong enrichment in several cores, such as D.C.C 1, Hinthorn CW-1, Edmonds 1-A, and Tietjens 1-12, but it is not present in PNR 1 or PNR 2 (table 37) and does not always show the highest concentrations. Other shale members — such as the Anna, Nuyaka Creek, Binkley, and Excello units — also show strong enrichment in certain cores. This means that metal enrichment is not restricted to a single vertical interval but instead reflects a combination of regional redox conditions and local depositional variations. These patterns show that critical mineral potential occurs across multiple shale units rather than being limited to one or two key horizons. Spatial variation among cores indicates that depositional conditions were not uniform across the basin. Higher ICP element averages in the Hinthorn CW-1, Edmonds 1-A, D.C.C 1, and Tietjens 1-12 cores suggest that these areas experienced more reducing conditions, stronger organic matter preservation, or greater degrees of water mass restriction during shale deposition. In contrast, lower enrichment levels in PNR 1 point to more open or better-circulated depositional environments. These spatial trends show that redox conditions controlled not only temporal patterns of enrichment but also geographic variability in critical mineral distribution.

The strong correspondence between ICP-derived trace metal enrichments, TOC values, and sulfur content indicates that organic matter and early diagenetic sulfur cycling were major drivers of metal sequestration. Shales with high TOC and moderate to high sulfur generally contain the greatest concentrations of redox-sensitive elements. Mineralogical analyses support these relationships. XRD results show that clay-rich and phosphate-bearing intervals coincide with enriched metal concentrations, and SEM-EDS observations reveal metals residing within fine-grained sulfide phases and phosphate particles. These findings indicate that depositional redox conditions and early diagenetic mineral formation were the dominant mechanisms controlling the incorporation and preservation of critical minerals.

Collectively, the geochemical, mineralogical, and organic geochemical data suggest that the Pennsylvanian shales examined in this study hold measurable potential as a resource target for vanadium, nickel, zinc, and molybdenum. The regional consistency of enrichment in specific shale members, combined with predictable spatial patterns, provides a strong foundation for future detailed evaluation of critical mineral resources in this part of the basin.

6. Acknowledgments

This work was supported by the U.S. Geological Survey under the Earth Mapping Resources Initiative Cooperative Agreement (Grant No. G23AC00093-00).

We are especially grateful to Susie Fagan for her exceptional review, editing, and continued support during preparation of this Open File Report. Her thoughtful feedback, careful editing, and attention to detail greatly improved the quality and organization of this publication.

We would also like to acknowledge the support of the Kansas Geological Survey Drill Core Library, especially Olivia Buchhorn, and Laboratory Program Director Rachel Smith. We thank Stephanie Weaver, Katy Bream, and Tim Shaban for their assistance with the development and organization of project-related web materials and online data resources associated with the broader multistate project. We also acknowledge Kolbe Andrzejewski for his assistance with preparation of the Kansas map throughout the project.

References

- Coveney, R. M., Leventhal, J. S., Glascock, M. D. and Hatch, J. R., 1987, Origins of metals and organic matter in the Mecca Quarry Shale Member and stratigraphically equivalent beds across the Midwest: *Economic Geology*, 82 (4), 915–933.
- Emsbo, P., McLaughlin, P. I., Breit, G. N., du Bray, E. A. and Koenig, A. E., 2015, Rare earth elements in sedimentary phosphate deposits: solution to the global REE crisis?: *Gondwana Research*, 27 (2), 776–785.
- Heckel, P. H., 2013, Pennsylvanian stratigraphy of Northern Midcontinent Shelf and biostratigraphy correlation of cyclothems: *Stratigraphy*, 10 (1–2), 3–39.
- Mastalerz, M., Cortland, E., Drobniak, A., Ames, P.R., and McLaughlin, P.I., 2020, Rare earth elements and yttrium in Pennsylvanian coals and shales in the eastern part of the Illinois Basin: *International Journal of Coal Geology*, v. 231, 103620.
- Layzell, A. L., Oborny, S., Hasiuk, F., Smith, J.; Contractors: Clark, R., Heckel, P., Joeckel, M., Mulvany, P., Bridges, D., Stanley, T. M., 2021. Pennsylvanian stratigraphic nomenclatural reconciliation in the midcontinent. U.S. Geological Survey, National Geologic Map Database (NGMDB). https://ngmdb.usgs.gov/Geolex/stratres/strat_coops#coop5
- Oborny, S., Andrzejewski, K., Schneider, B., Bream, K., Bream, B., Smith, R., Smith, J., Louis, D., Clark, R., Bancroft, A., Cramer, B., Hayman, N., Suriamin, F., Ganz, K., Seeger, C., Steele, A., Joeckel, M., and Lynn, W., 2025b. C_MC_SC_FC_B—Critical Minerals in Coaly Strata of the Cherokee-Forest City Basin. U.S. Department of Energy (DOE) Carbon Ore, Rare Earth and Critical Minerals (CORE-CM) Initiative for U.S. Basins. <https://netl.doe.gov/project-information?p=FE0032056>
- Olivetti, E. A., Ceder, G., Gaustad, G. G., and Fu, X., 2017, Lithium-ion battery supply chain considerations: Analysis of potential bottlenecks in critical metals: *Joule*, 1 (2), 229–243.
- Schmitz, M. D., and Davydov, V. I., 2012, Quantitative radiometric and biostratigraphic calibration of the Pennsylvanian—Early Permian (Cisuralian) time scale and pan-Euramerican chronostratigraphic correlation: *GSA Bulletin*, 124 (3-4), 549–577.
- Vine J. D., 1969, Geochemical investigations of some black shales and associated rocks: U.S. Geological Survey Bulletin, 1214-A.

Yang, J., Torres, M., McManus, J., Algeo, T. J., Hakala, J. A., and Verba, C., 2017, Controls on rare earth element distributions in ancient organic-rich sedimentary sequences: Role of post-depositional diagenesis of phosphorus phases: *Chemical Geology*, 466, 533–544.